On the prediction of unconfined compressive strength of silty soil stabilized with bottom ash, jute and steel fibers via artificial intelligence

Hamza Güllü and Halil İbrahim Fedakar*

Department of Civil Engineering, University of Gaziantep, 27310, Gaziantep, Turkey

Abstract.   The determination of the mixture parameters of stabilization has become a great concern in geotechnical applications. This paper presents an effort about the application of artificial intelligence (AI) techniques including radial basis neural network (RBNN), multi-layer perceptrons (MLP), generalized regression neural network (GRNN) and adaptive neuro-fuzzy inference system (ANFIS) in order to predict the unconfined compressive strength (*UCS*) of silty soil stabilized with bottom ash (BA), jute fiber (JF) and steel fiber (SF) under different freeze-thaw cycles (FTC). The dosages of the stabilizers and number of freeze-thaw cycles were employed as input (predictor) variables and the *UCS* values as output variable. For understanding the dominant parameter of the predictor variables on the *UCS* of stabilized soil, a sensitivity analysis has also been performed. The performance measures of root mean square error (RMSE), mean absolute error (MAE) and determination coefficient (R^2) were used for the evaluations of the prediction accuracy and applicability of the employed models. The results indicate that the predictions due to all AI techniques employed are significantly correlated with the measured *UCS* ($p \leq 0.05$). They also perform better predictions than nonlinear regression (NLR) in terms of the performance measures. It is found from the model performances that RBNN approach within AI techniques yields the highest satisfactory results (RMSE = 55.4 kPa, MAE = 45.1 kPa, and R^2 = 0.988). The sensitivity analysis demonstrates that the JF inclusion within the input predictors is the most effective parameter on the *UCS* responses, followed by FTC.

Keywords: freeze-thaw cycle; unconfined compressive strength; silty soil; artificial intelligence; sensitivity analysis; bottom ash; jute fiber; steel fiber

1. Introduction

Applicability of artificial intelligence on the prediction of unconfined compressive strength of silt soil treated with the stabilizers of bottom ash, jute fiber and steel fiber under different freeze thaw cycles (0, 1, 2 and 3) has been addressed in this article. Strength response of fine-grained soil (low-plasticity silt in this study) as a marginal soil has become a great concern in long time for the stabilization uses in pavement base courses, subbase courses, subgrades, road embankment, highway constructions and foundation bases as a supporting layer under buildings, etc. This concern of the strength has been overcome by the stabilization of the silt with the different stabilizers; the traditional ones (i.e., bottom ash, lime, fly ash, cement, etc.) and the non-traditional

---

∗Corresponding author, Ph.D., E-mail: hhifem@gmail.com

ones (i.e., fiber reinforcement, liquid stabilizer, etc.). Due to the contribution to the environment in the point of recycling, the researches are mostly recommended to employ the stabilizers from the industrial waste materials as a traditional stabilizer (Hossain and Mol 2011, Sivrikaya *et al*. 2014, Güllü and Girişken 2013). In recent years, bottom ash as an industrial by product has been very popular for the stabilization applications since it provides a promising cementitious property as well as pozzolanic reactions. Modification of the silt properties due to the bottom ash addition through cation exchange, flocculation, agglomeration and hydration process with the silica and alumina sheets could result in favorable engineering characteristics in the stabilization applications (Kayabali and Bulus 2000, Kim 2003, Rifai *et al*. 2009, Kim *et al*. 2011). In spite of the benefits from the traditional stabilizers to the stabilization of silt, the non-traditional stabilizers could be incorporated in the stabilizations to improve the engineering characteristics and performances, particularly for cold regions of country (Tutumluer *et al*. 2004, Güllü and Hazirbaba 2010, Hazirbaba and Güllü 2010). The incorporation of non-traditional stabilizers would become beneficial, since it is reported that large amount of traditional stabilizers is mostly required being more effective to considerably decrease frost heave due to the cold region conditions (Lambe and Kaplar 1971a, b). Moreover, fine-grained soils, especially in cold regions, could not be desirable as a stabilization material due to their frost susceptible nature as well as their tendency to significant ice segregation with higher moisture (Güllü and Hazirbaba 2010). Apart from the considerations in the cold regions, the stabilization with the alternative materials like the non-traditional stabilizers could contribute to the cost of construction project in the point of specialized equipment, skills of workmanship and locally availability of stabilizer (Tutumler *et al*. 2004). Fiber as a non-traditional stabilizer has been extensively researched to the soil stabilizations in the concern of strength response mostly resulted in favorable conclusions (see Hejazi *et al*. (2012) for the review in detail). Despite of the numerous researches, the jute and steel fibers among them have still been less observed for the stabilizations particularly composed of silt as a marginal soil. Moreover, the strength responses due to the jute and steel fibers have not been sufficiently studied by considering the effect of the freezing-thawing cycle. It is concluded from the past works that the jute fiber reduces maximum dry density while increases optimum moisture content of the compacted soil. Addition of 0.8% jute fiber with 10 mm long results in an increase in the strength value (CBR) more than 2.5 times compared to the strength value of native clay (Aggarwal and Sharma 2010, Islam and Iwashita 2010). As for the steel fibers, as well as their good reinforcement in the soil-cement composites, they are proposed to improve the soil strength, but this improvement requires more effort of study for confirmation of their effects (Gray and Al-Refeai 1986, Murray and Farrar 1988, Ghazavi and Roustaie 2010).

Since the strength is an important consideration in the stabilizations, development of prediction models depending on the stabilizer rates is always desired in practice for design of stabilization (Narendra *et al*. 2006, Kalkan *et al*. 2009). This prediction effort for the applications particularly in the cold regions would also be useful for a cost-benefit design as well as improving the engineering characteristics of stabilization. Moreover, the prediction models of strength could offer simpler and faster solutions to the construction of stabilization in the cases of routine test requirements and limited laboratory facilities (Tutumluer *et al*. 2004, Baykasoglu *et al*. 2008, Canakci *et al*. 2009). Due to the reasons arisen above, an effort to predict the unconfined compressive strength of silt stabilized with bottom ash, jute fiber and steel fiber under the freeze-thaw cycles has been attempted in this paper. However, in particular for the stabilizations composed of fine-grained soil, due to highly non-linear behavior, the strength prediction has still been questionable in the correlations and residuals when derived by a conventional method of

regression (Narendra *et al*. 2006). Moreover, especially for the applications considering the effect of freeze-thaw cycles on the fine-grained soil at cold regions (Ghazavi and Roustaie 2010), the nonlinearity of the soil behavior causes this prediction issue more complex when estimated via regression. Therefore, alternative techniques, artificial neural networks (ANNs) and adaptive neuro-fuzzy inference system (ANFIS), presenting new opportunities to the solution of nonlinear problems (Güllü and Erçelebi 2007, Kayadelen *et al*. 2009, Güllü 2012, 2013) have been applied in this paper in comparison with the regression.

The ANN and fuzzy system have become a remarkable subject of modeling for identifying the influence of the independent (i.e., input) variables into the dependent (i.e., output) variable in the data set of experiments even in the most complex systems of the underlying input-output relationship in uncertainty and imprecision (Kayadelen *et al*. 2009, Güllü 2013, Ellis *et al*. 1995, Akbulut *et al*. 2004, Stegemann and Buenfeld 2003, Erzin and Cetin 2014, Erzin and Gul 2013, Sivapullaiah *et al*. 2009). This has been carried out through the fitting of composite functions to the experimental data by modifying the parameters of component non-linear functions in an iterative "training process", which minimizes the residual between the predicted and measured outputs (Stegemann and Buenfeld 2003). For the soil modeling of different purposes, the applications of the ANN and fuzzy systems have been available in the literature increasingly (Narendra *et al*. 2006, Kayadelen *et al*. 2009, Ellis *et al*. 1995, Akbulut *et al*. 2004, Cal 1995, Levine *et al*. 1996, Najjar *et al*. 1996, Tutumluer and Seyhan 1998, Dayakar and Rongda 1999, Akbulut *et al*. 2003, Lee *et al*. 2003, Habibagahi and Bamdad 2003, Shahin *et al*. 2001, 2003, Sinha and Wang 2008, Yilmaz and Kaynar 2011). All the previous studies are relatively successful to model the soil behavior directly from experimental data due to the ability of artificial intelligence to learn and generalize the interactions among the variables. Tutumluer and Seyhan (1998) studied the ANN model for stress–strain relationships of granular materials through CD triaxial compression test data, and developed a successful simulation of nonlinear stress–strain behavior for lower strain levels that can be achieved using the ANN methodology. Habibagahi and Bamdad (2003) obtained a successful soil modeling due to the ANN technique for the characterization of mechanical behavior of unsaturated clays, in which they employed triaxial deformation measurements, deviatoric stress, volumetric deformation and suction pressure as the soil parameters. Akbulut *et al*. (2003) used the ANN for estimation of the shear strength from different grain size, moisture content and dry unit weight of soil samples, and found that the ANN technique are able to produce a reliable and simple prediction model for the shear strength of compacted soil samples. Goktepe *et al*. (2008) estimated the shear strength parameters of plastic clay on the basis of index properties using the neural network, and found that the ANN based model is superior as compared with regression. A different study performed by Kayadelen *et al*. (2009) presented the usage of artificial intelligence on the estimation of the internal friction angle of soil depending on the parameters of fine-grained percentage, coarse-grained percentage, liquid limit and bulk density. Yılmaz and Kaynar (2011) investigated the applicability of the ANN and ANFIS models for prediction of swell-potential of clayey soils. They found that radial basis function of the ANN exhibited a high performance than the regression for predicting the swell pressure, proposing the artificial intelligence techniques in the soil related problems for minimizing the uncertainties and the potential inconsistency of correlations.

In spite of the extensive applications for modeling of soil characteristics in the literature in various problems due to the artificial intelligence, the overview of these efforts indicates a lack of attempt on the prediction of unconfined compressive strength of silty soil treated with jute fiber, steel fiber and bottom ash under different freeze-thaw cycles. The study presented herein employs

the ANNs and ANFIS to forecast the unconfined compressive strength of silty soil as the output variable, in terms of the independent (i.e., input) variables including the number of freeze-thaw cycle and the dosage rates of bottom ash, jute fiber, and steel fiber. The prediction ability of artificial intelligence has also been compared with nonlinear regression. Moreover, sensitivity analysis has been applied in order to see the relative importance of input variables used for developing models. The database of predictions has been collected from the previous studies (Güllü and Khudir 2014, Khudir 2014). The understanding of the interactions between the soil strength and the inclusion rates (i.e., bottom ash, steel fiber and jute fiber) under the various freeze-thaw cycles could fairly contribute to design of stabilizations in practice in viewpoint of effective parameter of inclusion.

2. Data collection

For the construction of database in the model developments of artificial intelligence, the experimental data has been collected from the previous efforts (Güllü and Khudir 2014, Khudir 2014) that conducted extensive unconfined compressive strength (*UCS*) tests for treatment of silty soil under the freeze-thaw cycles of 0, 1, 2, and 3 (zero cycle means non-freezing-thawing tests). For the experimental study in detail the reader are referred to the corresponding studies (Güllü and Khudir 2014, Khudir 2014).

In summary of the experimental work (Güllü and Khudir 2014, Khudir 2014) including materials and testings briefly, the soil used is a fine-grained soil that is low-plasticity silt (ML) according to the Unified Soil Classification System (USCS). It has maximum dry-unit weight of 19 kN/m^3 and optimum moisture content of 18% which were determined from the compaction tests conducted in accordance with ASTM D-1557. The bottom ash as a soil stabilizer is supplied from a domestic coal-based plant. Its particle gradation is varying from 0.075 mm to 4.74 mm, which corresponds to the particle sizes of fine to coarse sand. The uniformity properties (i.e., C_u, C_c) show that the bottom ash is a poorly graded material (or uniformly-graded material). Table 1 presents some index and physical properties of soil and bottom ash used in the study. As for the fibers used (Fig. 1), the jute fiber was supplied from the carpet industry as a waste material. It has the length of 20-40 mm and the diameter of 1 mm with the specific gravity of 1.7. The steel fiber has the specific gravity of 7.85 and the length of 35 mm with the diameter of 5.5 mm. The dosage rates of both the jute and steel fibers used are 0.25%, 0.50%, 0.75% and 1.00% by dry weight of the soil. The mix proportions of bottom ash (by dry weight of the soil) are 10%, 20%, 30%, 40% and 50%.

As for the summary of testings, they all for the experimental data collected have been carried out for unsoaked conditions (i.e., where the adequate drainage and unsaturated conditions are provided) on the basis of the findings from previous studies (Güllü and Hazirbaba 2010, Hazirbaba and Güllü 2010). No curing conditions of samples were tested due to conservative side and time saving. Cylindrical specimens were prepared in the diameter of 55 mm and the height of 110 mm conforming to a minimum of 2:1 height to diameter ratio. Samples were mixed at the optimum water content of native soil (18%) and then compacted following the modified proctor energy (ASTM D-1557 2012) to the dry unit weight which is being minimum 95% of the maximum dry unit weight of native soil. *UCS* tests have been conducted in accordance with the procedure in ASTM D-2166 (2006). The compression loading machine is a universal testing machine with a maximum load capacity of 100 kN. The loading was continued to an axial strain of 35% for the

Table 1 Some index properties of soil and bottom ash (Khudir 2014)

Property	Silt	Bottom ash
Specific gravity	2.72	2.1
C_u	-	2
C_c	-	0.9
Liquid limit (%)	37	-
Plastic limit (%)	25	-
Plasticity index (%)	12	NP
Classification (USCS)	ML	SP
Maximum dry unit weight (kN/m^3)*	19	8.7
Optimum moisture content (%)*	18	18

NP: non-plastic, *Modified proctor

(a) Jute fiber	(b) Steel fiber

Fig. 1 Jute and steel fibers used by Güllü and Khudir (2014) and Khudir (2014)

jute fiber. For the remaining inclusions, the loading was continued until the failure or the load value indicates a decrease with an increasing strain. Thus, the *UCS* performance corresponds to the maximum (peak) stress attained.

As for the freezing-thawing tests, the closed-system freezing conditions (i.e., where no source of water is available during the freezing process beyond that originally in the voids of the soil) was applied (Jones 1987). For the freezing, the specimens in the freezing apparatus were subjected to the temperature of -18°C for 24 hr to obtain a complete frost penetration. Then, they were allowed to thaw at a temperature of 18°C for 24 hr in a room with the relative humidity of 100%. After the freezing and thawing process of the corresponding cycles (i.e., 0, 1, 2, 3), the specimens were performed for *UCS* testing.

3. Methodology

3.1 Artificial neural network (ANN)

The ANN approach is a computer methodology that attempts to simulate some important features of the human nervous system, in other words, the ability to solve problems by applying

information gained from past experience to new problems or case scenarios. Analogous to a human brain, the ANN uses many simple computational elements, named artificial neurons, connected by variable weights. The ANN modeling consists of two steps: to train and to test the network. During the training period, the network makes use of the inductive-learning principle to learn from a set of examples called the training set. Test data could not be used in training (Haykin 1998). Radial basis neural network (RBNN), multi-layer perceptrons (MLP) and generalized regression neural network (GRNN) approaches have been employed in the presented study.

3.1.1 Radial basis neural network (*RBNN*)

RBNN was introduced into the neural network literature by Broomhead and Lowe (1988). A RBNN model is motivated by the locally tuned response observed in biological neurons. Neurons with a locally tuned response characteristic can be found in several parts of the nervous system, for example, cells in the visual cortex sensitive to bars oriented in a certain direction or other visual features within a small region of the visual field (Poggio and Girosi 1990).

RBNN utilizes a clustering process on the input data before presentation to the network and different non-linear activation functions that are locally tuned to cover a region of the input space. The schematic diagram of RBNN structure shown in Fig. 2 consists of an input layer, a single hidden layer containing the same number of nodes as the cluster centers, and an output layer (Leonard *et al*. 1992).

The basis functions in the hidden layer produce a significant non-zero response to input stimulus only when the input falls within a small localized region of the input space. Hence, this paradigm is also known as a localized receptive field network (Lee and Chang 2003). Transformation of the inputs is essential for fighting the curse of dimensionality in empirical modeling. The type of input transformation of RBNN is the local nonlinear projection using a radial fixed shape basis function. After nonlinearly squashing the multi-dimensional inputs without considering the output space, the radial basis functions play a role as regressors. Since the output layer implements a linear regressor, the only adjustable parameters are the weights of this regressor. These parameters can therefore be determined using the linear least square method, which gives an important advantage for convergence (Gencel *et al*. 2013). More theoretical information on RBNN can be found in Kocabas and Unal (2010).
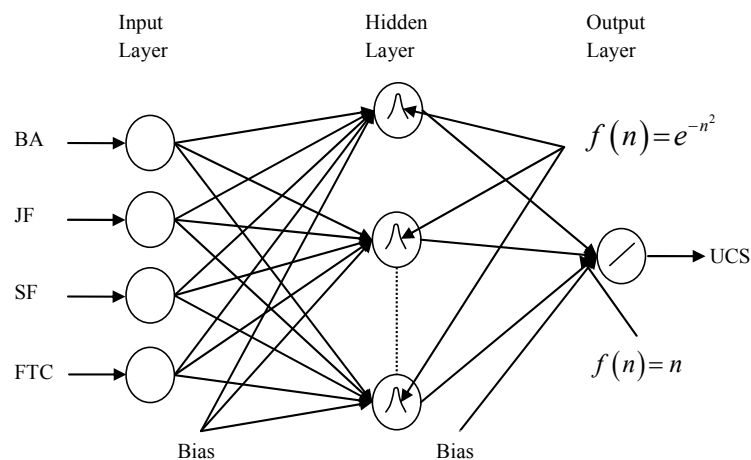

Fig. 2 Schematic diagram of RBNN structure

RBNN method does not perform parameter learning as in the back propagation networks, but just performs linear adjustment of the weights for the radial bases. This characteristic of RBNN gives the advantage of a very fast converging time without local minima, since its error function is always a convex (Kisi 2008, Kocabas and Unal 2010). In this study, different numbers of hidden neurons and spread coefficients are examined for the RBNN models (Kisi 2009).

3.1.2 Multi-layer perceptrons (MLP)

A MLP model has one or more hidden layers, whose computation nodes are correspondingly called hidden neurons of hidden units. The function of hidden neurons is to intervene between the external input and the network output in some useful manner. By adding one or more hidden layers, the network is enabled to extract higher order statistics. In a rather loose sense, the network acquires a global perspective despite its local connectivity due to the extra set of synaptic connections and the extra dimension of neural network interconnections. Detailed theoretical information about MLP can be found in Haykin (1998).

The network structure of a MLP model constitutes an input layer, a single hidden layer containing the same number of nodes as cluster centers, and an output layer. MLP can have more than one hidden layer; however theoretical work has shown that a single hidden layer is sufficient for an ANN to approximate any complex nonlinear function (Cybenco 1989, Homik *et al.* 1989). Therefore, a one-hidden-layer MLP was used in this paper. Throughout all MLP simulations adaptive learning rates were used to speed up training. The developed MLP models were trained using a Levenberg–Marquardt technique here because this technique is more powerful than the conventional gradient descent techniques (Hagan and Menhaj 1994, El-Bakyr 2003, Cigizoglu and Kisi 2005). While back propagation with gradient descent technique is a steepest descent algorithm, the Levenberg–Marquardt algorithm is an approximation to Newton's method (Marquardt 1963). More detailed information on Levenberg–Marquardt algorithm is available in Hagan and Menhaj (1994).

3.1.3 Generalized regression neural network (GRNN)

The basics of GRNN are given in Specht (1991) and Tsoukalas and Uhrig (1997). A GRNN model is composed of four layers: an input layer, a pattern layer, a summation layer, and an output layer. The number of input units in the first layer is equal to the total number of parameters. The first layer is fully connected to the second, pattern layer, where each unit represents a training pattern and its output is a measure of the distance of the input from the stored patterns. Each pattern layer unit is connected to two neurons in the summation layer: the S-summation neuron and the D-summation neuron. The S-summation neuron computes the sum of the weighted outputs of the pattern layer while the D-summation neuron calculates the unweighted outputs of the pattern neurons. For the D-summation neuron, the connection weight is unity. The output layer merely divides the output of each S-summation neuron by that of each D-summation neuron, yielding the predicted value to an unknown input vector x as

$$\widehat{y}_i(x) = \frac{\sum\limits_{i=1}^{n} y_i \exp[-D(x,x_i)]}{\sum\limits_{i=1}^{n} \exp[-D(x,x_i)]} \qquad (1)$$

where n indicates the number of training patterns and the Gaussian D function in Eq. (1) is defined as

$$D(x, x_i) = \sum_{j=1}^{p} \left(\frac{x_j - x_{ij}}{\zeta} \right)^2 \tag{2}$$

where p indicates the number of elements of an input vector. x_i and x_{ij} represent the jth element of x and x_i, respectively. The ζ is generally referred to as the spread factor, whose optimal value is often determined experimentally (Kim *et al*. 2003). GRNN method does not require an iterative training procedure as in MLP. GRNN is employed for estimation of continuous variables, as in standard regression techniques. It is related to the radial basis function network and is based on a standard statistical technique called kernel regression (Specht 1991). The joint probability density function (pdf) of x and y is estimated during a training process in GRNN. Because the pdf is derived from training data with no preconceptions about its form, the system is perfectly general. The success of a GRNN model depends heavily on the spread factors (Specht 1991, Wasserman 1993): the larger the spread, the smoother the function approximation. Too large a spread means a lot of neurons will be required to fit a fast changing function. Too small a spread means many neurons will be required to fit a smooth function, and the network may not generalize well.

3.2 Adaptive neuro-fuzzy inference system (ANFIS)

ANFIS approach, first introduced by Jang (1993), is a universal approximator and, as such, is capable of approximating any real continuous function on a compact set to any degree of accuracy (Unal *et al*. 2010). Therefore, in parameter prediction, where the given data are such that the system associates measurable system variables with an internal system parameter, a functional mapping may be constructed by ANFIS that approximates the process of estimation of the internal system parameter (Kiszka *et al*. 1985).

As a simple example, a fuzzy inference system with two inputs x and y and one output f is assumed. The first-order Sugeno fuzzy model, a typical rule set with two fuzzy If–Then rules can be expressed as (Kisi and Fedakar 2014)

$$\text{Rule 1:} \quad \text{IF } x \text{ is } A_1 \text{ AND } y \text{ is } B_1 \text{ THEN } \quad f_1 = p_1 x + q_1 y + r_1 \tag{3}$$

$$\text{Rule 2:} \quad \text{IF } x \text{ is } A_2 \text{ AND } y \text{ is } B_2 \text{ THEN } \quad f_2 = p_2 x + q_2 y + r_2 \tag{4}$$

Here, the output f is the weighted average of the individual rules outputs and is itself a crisp value. More information on ANFIS can be found in Jang (1993).

3.3 Sensitivity analysis

Sensitivity analysis on how input parameters are dominant on *UCS* has been performed using Weights method, which was suggested by Garson (1991) and repeated by Goh (1995). Weights method is a procedure for partitioning the connection weights to determine the relative importance of the different independent variables on dependent variable. This method basically contains partitioning the input-output connection weights of each hidden neuron into components related to each input neuron. Gevrey *et al*. (2003) proposed the following equations

$$Q_{ih} = \frac{|W_{ih}|}{\sum_{i=1}^{ni} |W_{ih}|} \tag{5}$$

$$RI(\%)_i = \frac{\sum_{h=1}^{nh} Q_{ih}}{\sum_{h=1}^{nh}\sum_{i=1}^{ni} Q_{ih}} x100 \tag{6}$$

where *ni* and *nh* stand for the number of input and hidden neurons, respectively. W_{ih} is the multiplication of input weight value by output weight value and *RI* is the relative importance of each independent variable.

4. Model development

Artificial neural networks (ANNs), namely radial basis neural network (RBNN), multi-layer perceptrons (MLP) and generalized regression neural network (GRNN), adaptive neuro-fuzzy inference system (ANFIS) and nonlinear regression (NLR) models have been used to forecast the *UCS* of silty soil treated with bottom ash (BA), jute fiber (JF), and steel fiber (SF) under freeze-thaw cycle (FTC). Therefore, *UCS* has been taken as a dependent variable and the percentages of bottom ash (BA), jute fiber (JF) and steel fiber (SF) and number of freeze-thaw cycles (FTC) as independent variables. Looney (1996) recommended 25% of data for testing. The data presented herein were employed in developing models. 49 experimental datasets were used. 37 data (approximately 75%) were selected to train the models and the remaining 12 data (approximately 25%) were selected to test the models. Since the testing dataset was not utilized for the training period, it could be strongly become a good indicator to test the accuracy of the models produced.

In order to assess and compare the results of the developed models, root mean square error (RMSE), mean absolute error (MAE) and determination coefficient (R^2) statistics were used. R^2 measures the degree to which two variables are linearly related. RMSE and MAE provide different types of information about the predictive capabilities of the model (Karunanithi *et al*. 1994). RMSE measures the goodness-of-fit relevant to high *UCS* values whereas MAE yields a more balanced perspective of the goodness-of-fit at moderate *UCS*. In the paper, RMSE was also taken into consideration as main evaluation criterion (Kisi 2009). RMSE, MAE and R^2 statistics are shown as

$$RMSE = \sqrt{\frac{1}{n}\sum_{j=1}^{n}\left[(UCS)_{measured,j} - (UCS)_{predicted,j}\right]^2} \tag{7}$$

$$MAE = \frac{1}{n}\sum_{j=1}^{n}\left|(UCS)_{measured,j} - (UCS)_{predicted,j}\right| \tag{8}$$

$$R^2 = \frac{\sum_{j=1}^{n}\left\{(UCS)_{measured,j} - (\overline{UCS})_{measured}\right\}^2 - \sum_{j=1}^{n}\left\{(UCS)_{measured,j} - (UCS)_{predicted,j}\right\}^2}{\sum_{j=1}^{n}\left\{(UCS)_{measured,j} - (\overline{UCS})_{measured}\right\}^2} \tag{9}$$

in which n is the number of data, *UCS* is the unconfined compressive strength and $\overline{UCS}$ is mean of the *UCS*.

In the present paper, different RBNN, MLP, GRNN, and ANFIS models were established using MATLAB language to predict *UCS*. The common trial and error method was used in order to find the best model that gave the lowest RMSE and MAE and the highest R^2 and its parameters (Kisi 2009).

Before applying RBNN, MLP and GRNN to the data, the training input and output values were normalized using the following equation

$$a\frac{x_i - x_{min}}{x_{max} - x_{min}} + b \tag{10}$$

where x_{min} and x_{max} denote the minimum and maximum values of the data set. Different values can be assigned for the scaling factors *a* and *b*. There are no fixed rules as to which standardization approach should be used in particular circumstances (Kisi 2009). Range of 0.2-0.8 increases the extrapolation ability of the ANN models (Kisi and Cobaner 2009, Cigizoglu 2003, Modi *et al.* 2003). Also, Cigizoglu (2003) showed that scaling input data between 0.2 and 0.8 gives the ANNs the flexibility to estimate beyond the training range. For this reason, the *a* and *b* were taken as 0.6 and 0.2 herein, respectively.

For RBNN analysis, different spread coefficients and number of hidden neurons which range from 0.1 to 2.0 and from 1 to 30 respectively was tried to obtain the best model that had minimum

Table 2 Statistical performance of RBNN models

Models	Training			Testing		
	RMSE (kPa)	MAE (kPa)	R^2	RMSE (kPa)	MAE (kPa)	R^2
RBNN (0.1, 7)	163.1	125.8	0.775	339.5	283.3	0.655
RBNN (0.2, 19)	90.3	59.5	0.931	105.3	81.8	0.938
RBNN (0.3, 17)	74.7	56.8	0.953	105.4	73.0	0.951
RBNN (0.4, 11)	87.4	65.1	0.935	65.8	55.5	0.979
RBNN (0.5, 15)	79.0	56.5	0.947	63.7	50.8	0.981
RBNN (0.6, 14)	76.0	54.5	0.951	60.6	48.6	0.984
RBNN (0.7, 18)	75.3	51.8	0.952	72.2	63.9	0.980
RBNN (0.8, 14)	83.3	57.8	0.941	65.4	53.8	0.981
RBNN (0.9, 14)	90.0	63.6	0.932	104.0	78.8	0.942
RBNN (1.0, 16)	81.1	57.3	0.944	89.7	73.4	0.962
RBNN (1.1, 15)	79.9	58.4	0.946	55.4	45.1	0.988
RBNN (1.2, 16)	74.2	49.9	0.953	58.8	52.2	0.987
RBNN (1.3, 10)	92.2	70.8	0.928	76.1	68.2	0.973
RBNN (1.4, 10)	92.4	71.0	0.928	76.4	68.3	0.973
RBNN (1.5, 13)	84.0	59.9	0.940	77.0	60.8	0.975
RBNN (1.6, 12)	94.6	69.7	0.924	89.6	65.0	0.959
RBNN (1.7, 14)	88.8	63.5	0.933	82.0	70.9	0.966
RBNN (1.8, 10)	106.1	78.1	0.905	86.4	53.3	0.958
RBNN (1.9, 10)	106.2	78.1	0.905	86.5	53.4	0.958
RBNN (2.0, 10)	106.4	78.2	0.904	86.6	53.5	0.958

Table 3 Statistical performance of MLP models

Models	Training			Testing		
	RMSE (kPa)	MAE (kPa)	R^2	RMSE (kPa)	MAE (kPa)	R^2
MLP (logsig, logsig,6)	20.7	14.7	0.996	63.1	48.5	0.987
MLP (tansig, tansig, 5)	72.9	49.2	0.955	83.8	63.8	0.963
MLP (purelin, purelin)	126.3	95.3	0.865	117.1	97.4	0.926
MLP (tansig, logsig, 6)	48.1	39.4	0.981	81.2	65.9	0.964
MLP (logsig, tansig, 7)	104.4	78.2	0.911	85.5	75.7	0.967
MLP (logsig, purelin, 5)	56.3	42.7	0.973	89.1	69.5	0.954
MLP (tansig, purelin, 8)	8.5	5.9	0.999	57.9	47.3	0.981
MLP (purelin, logsig)	123.5	93.2	0.871	119.6	97.6	0.920
MLP (purelin, tansig)	122.5	90.8	0.873	114.0	91.7	0.928

Table 4 Statistical performance of GRNN models

Models	Training			Testing		
	RMSE (kPa)	MAE (kPa)	R^2	RMSE (kPa)	MAE (kPa)	R^2
GRNN (0.10)	56.0	38.8	0.977	142.5	101.3	0.882
GRNN (0.11)	69.3	48.4	0.965	138.0	100.8	0.891
GRNN (0.12)	80.8	57.0	0.952	136.4	101.4	0.896
GRNN (0.13)	90.7	64.5	0.939	136.8	102.7	0.897
GRNN (0.14)	99.2	70.9	0.927	138.5	104.2	0.897
GRNN (0.15)	106.8	76.4	0.916	141.1	105.9	0.895
GRNN (0.16)	113.5	81.0	0.906	144.2	107.4	0.893
GRNN (0.17)	119.6	85.1	0.896	147.5	108.8	0.891
GRNN (0.18)	125.2	88.9	0.888	151.1	109.8	0.889
GRNN (0.19)	130.5	92.4	0.880	154.9	111.4	0.888
GRNN (0.20)	135.6	96.3	0.873	158.9	114.3	0.888
GRNN (0.30)	187.5	142.4	0.828	216.6	171.2	0.901
GRNN (0.40)	236.9	184.3	0.797	279.6	237.8	0.903
GRNN (0.50)	270.6	212.4	0.775	322.6	280.3	0.897
GRNN (0.60)	291.6	231.5	0.761	349.0	306.2	0.890
GRNN (0.70)	305.1	244.5	0.751	365.7	322.5	0.885
GRNN (0.80)	314.0	253.1	0.745	376.6	333.2	0.881
GRNN (0.90)	320.2	259.1	0.741	384.2	340.6	0.878
GRNN (1.00)	324.7	263.4	0.738	389.6	345.9	0.876

RMSE and MAE and maximum R^2. The developed RBNN models are given together with the statistical performances in training and testing periods in Table 2. In this table, RBNN (0.1, 7) denote a RBNN model with a spread coefficient of 0.1 and a number of neuron in hidden layer of 7. In order to develop the best MLP model, Levenberg-Marquardt backpropagation training function and different transfer functions for input and output were used to obtain the best model.

Table 5 Statistical performance of ANFIS models

Models	Training			Testing		
	RMSE (kPa)	MAE (kPa)	R^2	RMSE (kPa)	MAE (kPa)	R^2
ANFIS (3, Gaussmf, Constant)	53.6	32.1	0.976	61.6	50.9	0.980
ANFIS (3, Gauss2mf, Constant)	47.6	27.4	0.981	91.6	72.6	0.965
ANFIS (3, Gbellmf, Constant)	48.9	27.9	0.980	71.2	57.4	0.978
ANFIS (3, Pimf, Constant)	48.9	30.0	0.980	96.3	75.6	0.961
ANFIS (3, Trimf, Constant)	53.6	31.5	0.976	58.3	46.6	0.983
ANFIS (3, Trapmf, Constant)	50.0	30.4	0.979	94.9	78.2	0.957

The utilized transfer functions are log-sigmoid (logsig), hyperbolic tangent sigmoid (tansig) and linear (purelin). Additionally, various numbers of hidden nodes varying from 1 to 30 were tried. The best generated MLP models and their statistical performances in training and testing are presented in Table 3. In this table, for MLP (logsig, tansig, 7) model, the first term (logsig), second term (tansig) and last term (7) represent input and output transfer functions and number of hidden nodes, respectively. In GRNN analysis, different spread coefficients between 0.1 and 1 were employed to find the one that showed minimum RMSE and MAE and maximum R^2 for the given problem. The produced GRNN models with the evaluation statistics are given in Table 4. In this table, GRNN (0.10) indicates a GRNN model has a spread coefficient of 0.10. For the ANFIS applications, different membership functions and a different number of membership functions (2 and 3) were utilized. The employed membership functions are gaussian curve built-in (gaussmf), gaussian combination (gauss2mf), generalized bell-shaped built-in (gbell), π-shaped built-in (pimf), triangular-shaped built-in (trimf), and trapezoidal-shaped built-in (trapmf) for input and constant and linear for output. The best developed ANFIS models for each input membership function are presented along with their statistical performances in training and testing in Table 5. In this table, ANFIS (3, Gaussmf, Constant) shows an ANFIS model having three gaussian curve built-in membership functions and constant output membership function. The results of statistical performances of the developed AI models will be discussed in the next section.

The nonlinear regression (NLR) finds a nonlinear model between independent and dependent variables. Therefore, in this study, nonlinear regression has been carried out on the 37 experimental data and tested using the remaining 12 data in order to determine the relationship between four independent variables and *UCS* testing results. Also, since nonlinear regression (NLR) is a method that is commonly used for prediction, the statistical performances of the developed AI models will be compared with those of NLR in the next section.

5. Results and discussion

The statistical parameters of BA, JF, SF, FTC and *UCS* for training, testing and whole datasets are given in Table 6. In this table, the x_{mean}, S_x, C_v, C_{sx}, x_{max} and x_{min} demonstrate the mean, standard deviation, variation and skewness coefficients, maximum and minimum, respectively. It is clear from the table that the distributions of BA, JF, SF and FTC are highly skewed, moderately skewed, highly skewed and approximately symmetric respectively for all datasets. While showing a moderately skewed distribution for the training and testing data, *UCS* shows an approximately

symmetric distribution for whole data. Dependent and independent variables show high variations for all data sets. It can be said from Table 6 that JF parameter has the highest magnitude of correlation coefficient, while BA parameter has the lowest magnitude. In addition, following JF, the parameters having the highest magnitude are SF and FTC, respectively. As regard to the correlation coefficient of the datasets, Rumsey (2011) suggested the following guide for the values of correlation coefficient (R): (i) If a model has $|R| = 1$, a perfect correlation exists between input variable (BA, JF, SF, and FTC) and output variable (UCS). (ii) If a model has $|R| = 0.70$, a strong correlation exists between input variable and output variable. (iii) If a model has $|R| = 0.50$, a moderate correlation exists between input variable and output variable. (iv) If a model has $|R| = 0.30$, a weak correlation exists between input variable and output variable. (v) If a model has $|R| = 0$, no correlation exists between input variable and output variable. For the negative values of correlation coefficient, it is said that there is a negative or downhill correlation that means as input (independent) variable increases, output (dependent) variable decreases. According to the suggestions by Rumsey (2011), the results in Table 6 imply that the inclusion of jute fiber to the natural soil in this paper produced the highest correlation with UCS, on which the magnitude qualitatively defined as "strong to perfect". This is followed by variable SF with the magnitude association of "weak to moderate". Bottom ash and freeze-thaw cycle have weak correlation with UCS.

The results of the RBNN, MLP, GRNN and ANFIS models together with statistical performance criteria for both training and testing periods are given in Tables 2-5, respectively. While the learning capability of the developed models is determined during the training period, the performance of the model developed in the training period is always evaluated during the testing period that indicates the generalization capability of the model to be applicable in practice (Güllü

Table 6 Statistical parameters of each data set

Dataset	Data type	x_{mean}	S_x	C_v (S_x / x_{mean})	C_{sx}	x_{max}	x_{min}	Correlation with UCS
Training	BA (%)	5.946	10.661	1.793	1.629	40	0	-0.130
	JF (%)	0.264	0.363	1.377	0.937	1	0	0.868
	SF (%)	0.223	0.332	1.490	1.335	1	0	-0.337
	FTC	1.297	1.222	0.942	0.259	3	0	-0.104
	UCS (kPa)	612.730	348.559	0.569	0.772	1450	114	1.000
Testing	BA (%)	7.500	15.448	2.060	2.275	50	0	-0.168
	JF (%)	0.271	0.376	1.389	0.984	1	0	0.958
	SF (%)	0.229	0.345	1.504	1.424	1	0	-0.462
	FTC	1.500	1.000	0.667	0.000	3	0	-0.386
	UCS (kPa)	587.500	430.120	0.732	0.819	1485	126	1.000
Whole	BA (%)	7.432	11.355	1.528	1.392	50	0	0.034
	JF (%)	0.297	0.369	1.242	0.607	1	0	0.819
	SF (%)	0.189	0.283	1.496	1.661	1	0	-0.358
	FTC	1.297	1.167	0.900	0.242	3	0	-0.219
	UCS (kPa)	693.189	363.868	0.525	0.345	1485	114	1.000

2014). Hence, the error performances of the models in the testing period have been considered for the discussion. RMSE, MAE and R^2 statistics should be taken into consideration with together in order to make a decision the best model. As the training data set is not utilized for the testing period, it can be seen from the determination coefficients presented in Tables 2-5 that there is no overfitting in the developed AI models. This situation enhances the quality of the generated models and provides with robust estimations of unconfined compressive strength. As for RBNN model parameters, the best number of hidden neurons for each spread coefficient is given in Table 2. It can be generally seen from Table 2 that the numbers of hidden neurons are not in a regular trend (decreased or increased) with the evaluation criteria of the generated RBNN models and vary between 7 and 19. For MLP analysis, the best parameters obtained per trial are presented in Table 3. This table shows that when purelin transfer function is employed in hidden layer, MLP models give the worst predictions with regard to statistical performance. But the use of this transfer function in output layer makes better estimations that have less RMSE and MAE and higher R^2. The best neuron number in hidden layer is found to be between 5 and 8. It can be clear from the results of GRNN models given in Table 4 that spread coefficient is between 0.11 and 0.14 for the optimal solution of this type of problem. Table 4 also shows that increase in the spread value gives rise to an increment in RMSE and MAE statistics. As for ANFIS parameters, three membership functions and constant as output membership function are suggested to be utilized based on the results presented in Table 5. These findings may be explained via highly nonlinear problem taken into consideration in the presented study.

As respects the performance assessment of the developed AI models, Ferguson (2009) proposed the following guide for the values of determination coefficient (R^2): (i) If a model yields $R^2 = 0.04$, there is a minimum relationship between the estimated and measured values. (ii) If a model yields $R^2 = 0.25$, there is a moderate relationship between the estimated and measured values. (iii) If a model yields $R^2 = 0.64$, there is a strong relationship between the estimated and measured values. As the testing periods considered, the R^2 values of the built AI models presented in Tables 2-5 range from 0.655 to 0.988, which means that the AI models for *UCS* results in the relationships with reasonable performance demonstrating strong level. It is well known that only R^2 value is not a good indicator of estimation accuracy of a developed model. The reason of this is that R^2 value may not change by variation of dependent variable values of a model equally. Consequently, the statistical performances of error in the developed models should be considered as well as R^2. It can be deduced from this that lower error values with higher R^2 often show a more precise forecasting. It is seen from the developed RBNN models presented in Table 2 that the RBNN (1.1, 15) model has the lowest RMSE and MAE and the highest R^2 values of 55.4 kPa, 45.1 kPa, and 0.988, respectively. For the MLP models, while MLP (logsig, logsig, 6) has maximum R^2 value of 0.987, MLP (tansig, purelin, 8) has minimum RMSE and MAE values of 57.9 kPa and 47.3 kPa, respectively. As for the GRNN models, GRNN (0.40) has the highest R^2 value of 0.903. As the developed GRNN models are investigated in terms of RMSE and MAE statistics, it is found that GRNN (0.12) and GRNN (0.11) models have the smallest RMSE value of 136.4 kPa and MAE value of 100.8 kPa, respectively. From the statistically evaluation of the built ANFIS models, it can be said that ANFIS (3, Trimf, Constant) model has the lowest RMSE and MAE values of 58.3 kPa and 46.6 kPa, respectively and the highest R^2 value of 0.983. It is evident from Tables 2-5 that errors in most of RBNN, MLP and ANFIS models relatively make good estimations with an acceptable degree of accuracy. Based on the performance strategy discussed above (i.e., the models with lower RMSE and MAE and higher R^2) and the main evaluation criterion (RMSE) described in the previous section, it is made decision that RBNN (1.1, 15), MLP (tansig, purelin, 8

Table 7 Statistical performance and *p*-value of the best AI models and NLR model

Model inputs	Model output	Model	RMSE (kPa)	MAE (kPa)	R^2	*p*-value
BA JF SF FTC	*UCS* (kPa)	RBNN (1.1, 15)	55.4	45.1	0.988	0.000
		MLP (tansig, purelin, 8)	57.9	47.3	0.981	0.000
		GRNN (0.12)	136.4	101.4	0.896	0.000
		ANFIS (3, Trimf, Constant)	58.3	46.6	0.983	0.000
		NLR	13714.8	97.4	0.926	0.000

GRNN (0.12) and ANFIS (3, Trimf, Constant) models are found the best performed ones among the developed RBNN, MLP, GRNN, and ANFIS models. Herein, it should be noted that all input variables (BA, JF, SF, and FTC) used in the evolutions are included via the generated models.

The predictive ability of the best AI models and nonlinear regression model is given in Table 7. For the models presented in this table, the *p*-values have also been estimated at the significance level of 5%, which is commonly employed in practice. A small numerical *p*-value (< 0.05) shows a statistically significant relationship, whereas a large *p*-value (> 0.05) demonstrates that there is not a statistically relationship. The estimated *p*-values are given together with the statistical

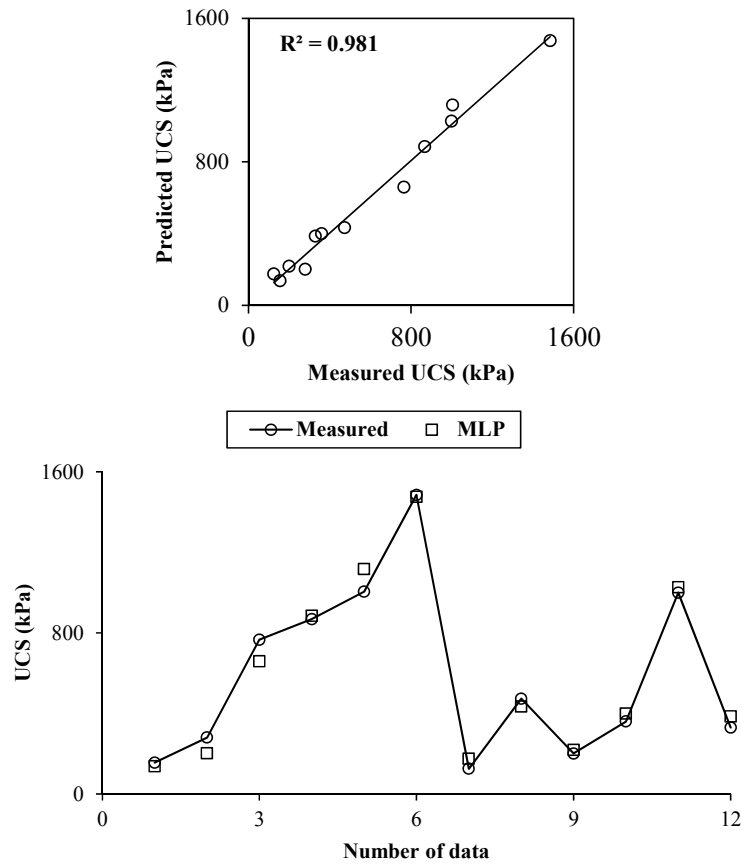Fig. 3 Comparison between predicted (by RBNN) and measured values of *UCS*

Fig. 4 Comparison between predicted (by MLP) and measured values of *UCS*

performances of models in Table 7. As seen from Table 7, the AI and NLR models provide a statistically significant fitting of relationship ($p < 0.05$) between the predicted and measured values of *UCS*. Also, it is clear from this table that even though NLR has lower MAE and higher R^2 than GRNN model, as having the highest RMSE, NLR makes the worst prediction among the developed models. Among the produced AI models, GRNN gives the worst estimation. Hence, between the AI methods used in the study, RBNN, MLP and ANFIS models can be proposed for prediction of unconfined compressive strength of silty soil stabilized with bottom ash, jute fiber and steel fiber under freeze-thaw cycles. Moreover, these models provide a good ability deliver accurate predictions for the training dataset. Additionally, when examined the results of the models in the viewpoint of the evaluation criteria used, RBNN makes slightly closer prediction to the measured *UCS* than MLP and ANFIS. Estimated *UCS* values obtained with the AI and NLR methods are graphically compared with the measured *UCS* values in Figs. 3-7. As seen from the figures, for the peak values of *UCS* ($\geq$ 800 kPa) the predictions of RBNN, MLP and ANFIS models are closer to the measured value of *UCS*. In addition to this, these models are well-graded with actual *UCS*. Also, it is seen from the figures that NLR model gives closer estimate to exact fit line with higher R^2 than GRNN model.

In order to examine the sensitivity of the *UCS* to the inputs and to gain an insight into which independent variable is the most effective parameter in the determination of *UCS* via the best
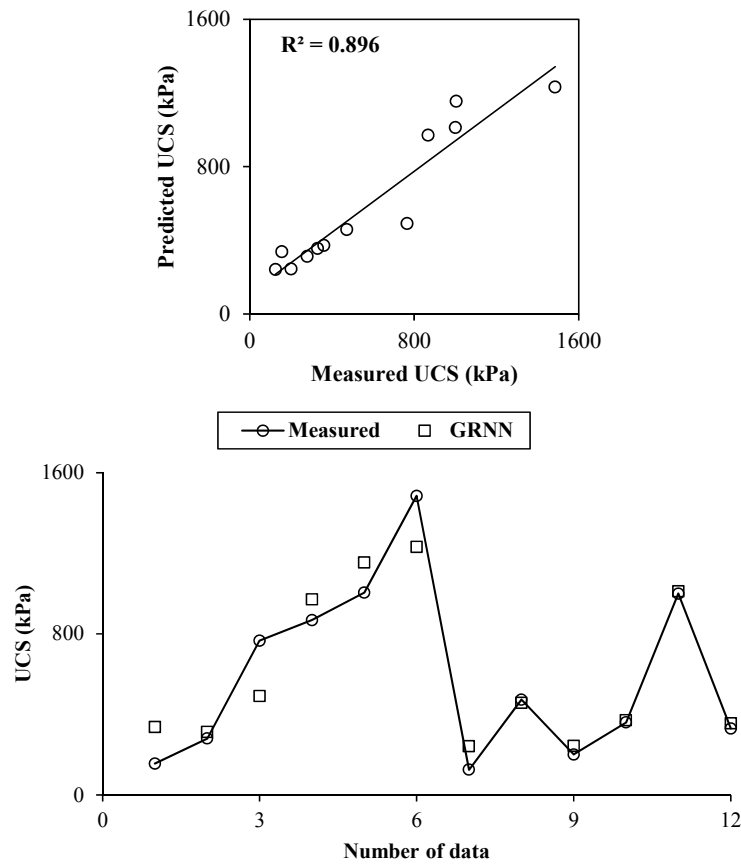
Fig. 5 Comparison between predicted (by GRNN) and measured values of *UCS*

model, sensitivity analysis has been carried out on RBNN (1.1, 15) output using Weights method. The connection weights of RBNN (1.1, 15) model are given in Table 8. The relative contribution (or % contribution) of each input parameter has been calculated using the weight values presented in Table 8. The results of sensitivity analysis are shown in Fig. 8. As can be seen from Fig. 8, jute fiber is found to be the most effective parameter in the prediction of *UCS*. It is followed by freeze-thaw cycle variable that has a close relative contribution to jute fiber. Bottom ash and steel fiber has the lowest contribution to strength, which are equal to each other in magnitude. The reason to be the most effective variable of jute fiber on the *UCS* may be attributed to the frictional interactions of jute fiber and soil. Since jute fiber is generally stronger and stiffer than the natural soil, the deformation is resisted by the jute fiber in the direction of the tensile strength by frictional interaction between jute fiber and soil (Güllü and Khudir 2014). Güllü and Khudir (2014) found that the contributions of steel fiber are lower than the ones of jute fiber. As for freeze-thaw cycle, most of the engineering properties (e.g., strength) of soils are severely affected by freezing-thawing period (Zaimoglu 2010). Here, an emphasis should be given that the results of sensitivity analyses represent the composition due to 4 parameters (BA, JF, SF and FTC). However, for a strong deduction of the parameter in most prominent to the strength, they should be tried in different combinations (i.e., (BA, SF, FTC), (BA, JF, FTC), (JF, SF, FTC), etc.), which is a separate topic of investigation for future work.
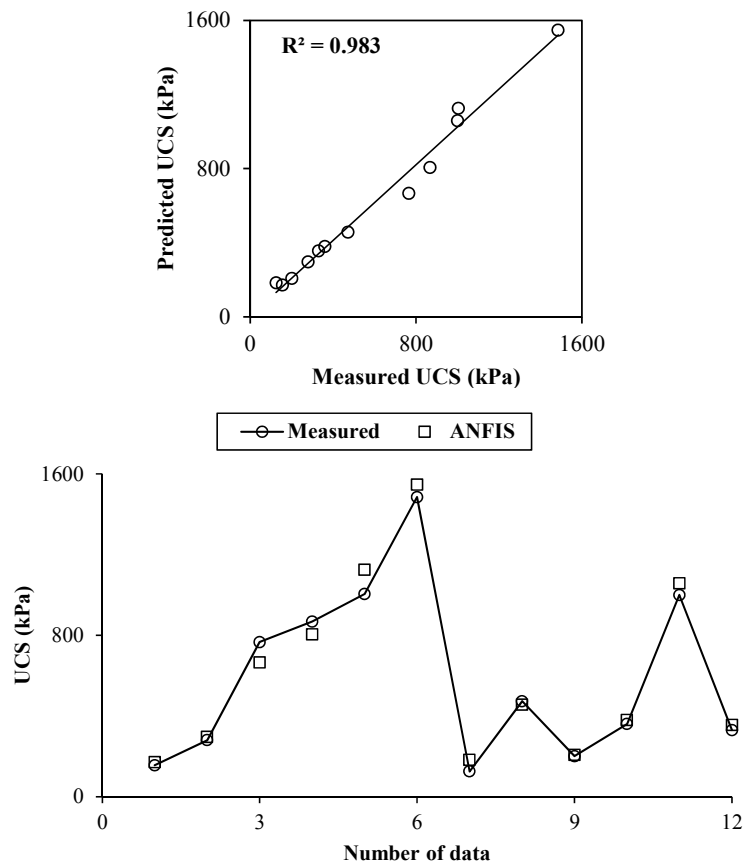
Fig. 6 Comparison between predicted (by ANFIS) and measured values of *UCS*

It should be noted that the proposed models are usually able to estimate within the data set employed for developing models. If more data become available, the models can be advanced in order to make the estimations for a wider data range. Here, it is important to note that the
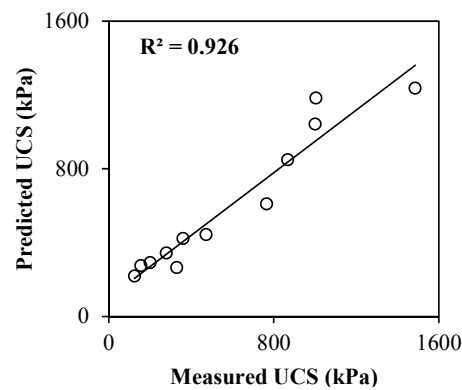

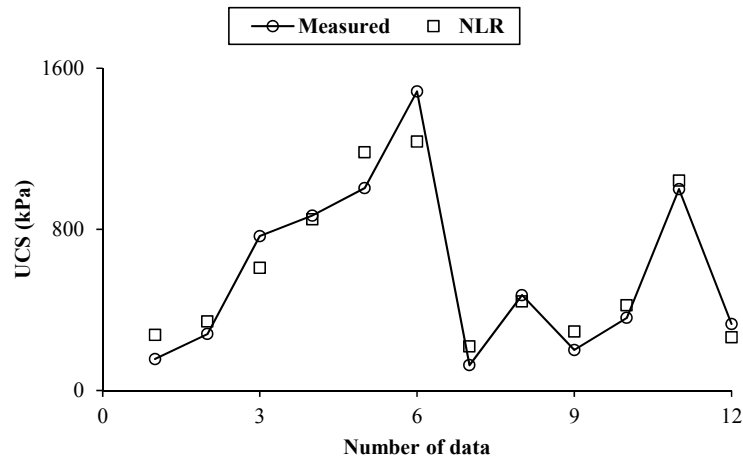Fig. 7 Comparison between predicted (by NLR) and measured values of *UCS*

Fig. 7 Continued

importance of engineering judgment in the interpretation of the estimated *UCS* values should be taken into consideration in practice. The estimations obtained from the developed models can be usually valid for use in preliminary design states and cautiously be employed for the final decision-making.

Considering *UCS* tests to be time consuming and expensive, it can emphasized the using artificial intelligence techniques for predicting *UCS*, in terms of the percentages of the stabilizers utilized and the number of freeze-thaw cycle, could be a beneficial tool to be employed for preliminary identification of material or/and a base of judgment for applicability of the *UCS* values.

Table 8 Connection weights of RBNN (1.1, 15) model

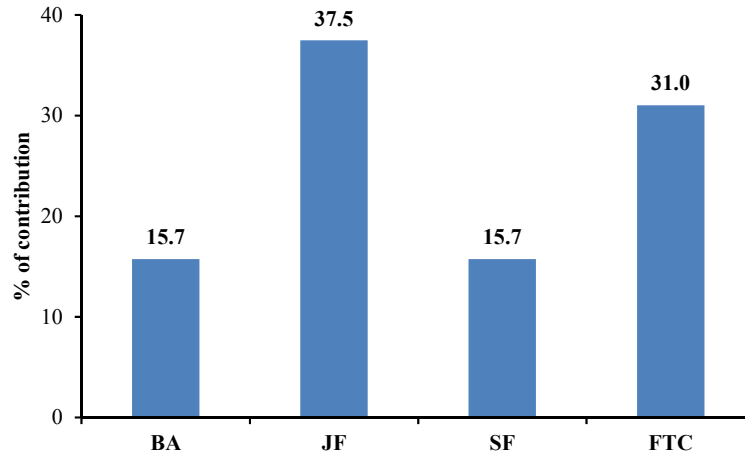| Number of hidden neuron	Weights input layers				Weights output layer
	BA	JF	SF	FTC	
1	0.2	0.8	0.2	0.2	1364.64625665502
2	0.2	0.5	0.2	0.2	-6280.40269528205
3	0.2	0.2	0.8	0.2	3.98433611024
4	0.2	0.2	0.8	0.4	-3.80891139955
5	0.2	0.8	0.2	0.8	-1477.52223089464
6	0.2	0.2	0.2	0.4	2092.22842915382
7	0.2	0.2	0.2	0.2	-5068.29529355041
8	0.2	0.35	0.2	0.2	9919.71825318400
9	0.5	0.2	0.35	0.8	2.26282075317
10	0.2	0.5	0.2	0.6	-7746.45387028618
11	0.5	0.65	0.2	0.8	-1.82097901553
12	0.2	0.8	0.2	0.4	-1487.00575750704
13	0.2	0.5	0.2	0.8	1410.38197360746
14	0.2	0.65	0.2	0.6	7829.12853651845
15	0.2	0.65	0.2	0.4	-565.77424365523

Fig. 8 Sensitivity analysis of RBNN output

6. Conclusions

In this paper, artificial intelligence techniques, namely RBNN, MLP, GRNN and ANFIS, and NLR method have been used in the estimation of the *UCS* of silty soil treated with bottom ash, jute fiber steel fiber under freeze-thaw cycles, with the investigation of their accuracy and applicability. In the construction of AI models (RBNN, MLP, GRNN, ANFIS and NLR), input parameters were established by BA, JF, SF and FTC, during the prediction of *UCS* as output variable. Performances of the models were examined using RMSE, MAE and R^2 statistics. Moreover, sensitivity analysis has been performed for the best model of AI, in order to understand the most prominent parameter of the input variables on the *UCS*. On the basis of the evaluations due to the performances of the model developments and sensitivity analysis, the following conclusions could be drawn from the present study.

- As compared with regression performances, RBNN, MLP, GRNN and ANFIS approaches are found to be more able to learn the relationship between input and output variables, and thus could be employed for forecasting of the *UCS* of silty soil treated with bottom ash, jute fiber and steel fiber under freeze thaw cycles.
- Comparing with measured data, the predicted *UCS* responses by the all AI methods yield statistically significant results ($p < 0.05$), which imply that all AI model employed for the present case of the study are applicable.
- Among the AI methods, RBNN is found to perform better results (RMSE = 55.4 kPa, MAE = 45.1 kPa, and $R^2 = 0.988$).
- Sensitivity analysis demonstrates that JF is the most prominent parameter (37.5%) on the contribution to *UCS*. This is followed by FTC (31%), BA (15.7%), and SF (15.7%), respectively.

Acknowledgments

carefully reviewing the manuscript and providing valuable comments.

References

Aggarwal, P. and Sharma, B. (2010), "Application of jute fiber in the improvement of subgrade characteristics", *Proceedings of 9th International Congress on Advances in Civil Engineering*, Trabzon, Turkey, September.

Akbulut, S., Kalkan, E. and Celik, S. (2003), "Artificial Neural Networks to estimate the shear strength of compacted soil samples", *International Conference on New Developments in Soil Mechanics and Geotechnical Engineering*, Lefkosa, TRNC, May.

Akbulut, S., Hasiloglu, A.S. and Pamukcu, S. (2004), "Data generation for shear modulus and damping ratio in reinforced sands using adaptive neuro-fuzzy inference system", *Soil Dyn. Earthq. Eng.*, **24**(11), 805-814.

ASTM D-1557 (2012), Standard Test Methods for Laboratory Compaction Characteristics of Soil Using Modified Effort.

ASTM D-2166 (2006), Standard Test Method for Unconfined Compressive Strength of Cohesive Soil.

Baykasoglu, A., Güllü, H., Canakci, H. and Özbakır, L. (2008), "Prediction of compressive and tensile strength of limestone via genetic programming", *Expert. Syst. Appl.*, **35**(1-2), 111-123.

Broomhead, D.S. and Lowe, D. (1988), "Multi-variable functional interpolation and adaptive networks", *Complex Syst.*, **2**, 321-355.

Cal, V. (1995), "Soil classification by neural-network", *Adv. Eng. Softw.*, **22**(2), 95-97.

Canakci, H., Baykasoglu, A. and Güllü, H. (2009), "Prediction of compressive and tensile strength of Gaziantep basalts via neural networks and gene expression programming", *Neural Comput. Appl.*, **18**, 1031-1041.

Cigizoglu, H.K. (2003), "Estimation, forecasting and extrapolation of river flows by artificial neural networks", *J. Hydrol. Sci.*, **48**(3), 349-361.

Cigizoglu, H.K. and Kisi, O. (2005), "Flow prediction by three back propagation techniques using k-fold partitioning of neural network training data", *Nordic Hydrol.*, **36**(1), 49-64.

Cybenco, G. (1989), "Approximation by superposition of a sigmoidal function", *Math. Control Signals Syst.*, **2**(4), 303-314.

Dayakar, P and Rongda, Z. (1999), "Triaxial compression behavior of sand and gravel using artificial neural networks (ANN)", *Comput. Geotech.*, **24**(3), 207-230.

Ellis, G.W., Yao, C., Zhao, R. and Penumadu, D. (1995), "Stress strain modeling of sands using artificial neural networks", *ASCE J. Geotech. Eng.*, **121**(5), 429-435.

El-Bakyr, M.Y. (2003), "Feed forward neural networks modelling for K-P interactions", *Chaos Solitons Fractals*, **18**(5), 995-1000.

Erzin, Y. and Cetin, T. (2014), "The prediction of the critical factor of safety of homogeneous finite slopes subjected to earthquake forces using neural networks and multiple regressions", *Geomech. Eng., Int. J.*, **6**(1), 1-15.

Erzin, Y. and Gul, T.O. (2013), "The use of neural networks for the prediction of the settlement of pad footings on cohesionless soils based on standard penetration test", *Geomech. Eng., Int. J.*, **5**(6), 541-564.

Ferguson, C.J. (2009), "An effect size primer: A guide for clinicians and researchers", *Prof. Psychol.: Res. Pract.*, **40**(5), 532-538.

Garson, G.D. (1991), "Interpreting neural network connection weights", *AI Expert*, **6**, 47-51.

Gencel, O., Koksal, F., Sahin, M., Durgun, M.Y., Hagg Lobland, H.E. and Brostow, W. (2013), "Modeling of thermal conductivity of concrete with vermiculite by using artificial neural network approaches", *Exp. Heat Transf.*, **26**(4), 360-383.

Gevrey, M., Dimopoulos, I. and Lek, S. (2003), "Review and comparison of methods to study the contribution of variables in artificial neural network models", *Ecol. Model.*, **160**(3), 249-264.

Ghazavi, M. and Roustaie, M. (2010), "The influence of freeze–thaw cycles on the unconfined compressive

strength of fiber-reinforced clay", *Cold Reg. Sci. Technol.*, **61**(2-3), 125-131.

Goh, A.T.C. (1995), "Back-propagation neural networks for modeling complex systems", *Artif. Intell. Eng.*, **9**(3), 143-151.

Goktepe, A.B., Altun, S., Altintas, G. and Tan, O. (2008), "Shear strength estimation of plastic clays with statistical and neural approaches", *Build. Environ.*, **43**(5), 849-860.

Gray, H. and Al-Refeai, T. (1986), "Behavior of fabric versus fiber reinforced sand", *ASCE J. Geotech. Eng.*, **112**(8), 804-820.

Güllü, H. (2012), "Prediction of peak ground acceleration by genetic expression programming and regression: A comparison using likelihood-based measure", *Eng. Geol.*, **141-142**, 92-113.

Güllü, H. (2013), "On the prediction of shear wave velocity at local site of strong ground motion stations: an application using artificial intelligence", *Bull. Earthq. Eng.*, **11**(4), 969-997.

Güllü, H. (2014), "Function finding via genetic expression programming for strength and elastic properties of clay treated with bottom ash", *Eng. Appl. Artif. Intell.*, **35**, 143-157.

Güllü, H. and Erçelebi, E. (2007), "A neural network approach for attenuation relationships: An application using strong ground motion data from Turkey", *Eng. Geol.*, **93**(3-4), 65-81.

Güllü, H. and Girişken, S. (2013), "Performance of fine-grained soil treated with industrial wastewater sludge", *Environ. Earth Sci.*, **70**(2), 777-788.

Güllü, H. and Hazirbaba, K. (2010), "Unconfined compressive strength and post-freeze–thaw behavior of fine-grained soils treated with geofiber and synthetic fluid", *Cold. Reg. Sci. Technol.*, **62**(2-3), 142-150.

Güllü, H. and Khudir, A. (2014), "Effect of freeze-thaw cycles on unconfined compressive strength of fine-grained soil treated with jute fiber, steel fiber and lime", *Cold Reg. Sci. Technol.*, **106-107**, 55-65.

Habibagahi, G. and Bamdad, A. (2003), "A neural network framework for mechanical behavior of unsaturated soils", *J. Can. Geotech.*, **40**(3), 684-693.

Hagan, M.T. and Menhaj, M.B. (1994), "Training feed forward networks with the Marquardt algorithm", *IEEE Trans. Neural Netw.*, **5**(6), 989-993.

Hazirbaba, K. and Güllü, H. (2010), "California bearing ratio improvement and freeze–thaw performance of fine-grained soils treated with geofiber and synthetic fluid", *Cold. Reg. Sci. Technol.*, **63**(1-2), 50-60.

Haykin, S. (1998), *Neural networks*: *A Comprehensive Foundation*, (2nd Edition), Prentice-Hall, Upper Saddle River, NJ, USA.

Hejazi, S.M., Sheikhzadeh, M., Abtahi, S.M. and Zadhoush, A. (2012), "A simple review of soil reinforcement by using natural and synthetic fibers", *Constr. Build. Mater.*, **30**, 100-116.

Hornik, K., Stinchcombe, M. and White, H. (1989), "Multilayer feed forward networks are universal approximators", *Neural Netw.*, **2**(5), 359-366.

Hossain, K.M.A. and Mol, L. (2011), "Some engineering properties of stabilized clayey soils incorporating natural pozzolans and industrial wastes", *Constr. Build. Mater.*, **25**(8), 3495-3501.

Islam, M. and Iwashita, K. (2010), "Earthquake resistance of adobe reinforced by low cost traditional materials", *J. Nat. Disaster Sci.*, **32**(1), 1-21.

Jang, J.S.R. (1993), "ANFIS: adaptive network based fuzzy inference system", *IEEE Trans. Syst. Manag. Cybern.*, **23**(3), 665-685.

Jones, C.W. (1987), "Long term changes in the properties of soil linings for canal seepage control", Report No. REC-ERC-87-1; U.S. Department of the Interior, Bureau of Reclamation, Engineering and Research Center, Denver, CO, USA.

Kalkan, E., Akbulut, S., Tortum, A. and Celik, S. (2009), "Prediction of the unconfined compressive strength of compacted granular soils by using inference systems", *Environ. Geol.*, **58**(7), 1429-1440.

Karunanithi, N., Grenney, W.J., Whitley, D. and Bovee, K. (1994), "Neural networks for river flow prediction", *ASCE J. Comput. Civ. Eng.*, **8**(2), 201-220.

Kayabali, K. and Bulus, G. (2000), "The usability of bottom ash as an engineering material when amended with different matrices", *Eng. Geol.*, **56**(3-4), 293-303.

Kayadelen, C., Günaydın, O., Fener, M., Demir, A. and Özvan, A. (2009), "Modeling of the angle of shearing resistance of soils using soft computing systems", *Expert Syst. Appl.*, **36**(9), 11814-11826.

Khudir, A. (2014), "Effect of freeze-thaw cycles on the strength of fine-grained soil stabilized with bottom

ash, lime, jute fiber and steel fiber", M.Sc. Dissertation; University of Gaziantep, Gaziantep, Turkey.

Kim, B. (2003), "Properties of coal ash mixtures and their use in highway embankments", Ph.D. Dissertation; Purdue University, West Lafayette, IN, USA.

Kim, B., Kim, S. and Kim, K. (2003), "Modelling of plasma etching using a generalized regression neural network", *Vac.*, **71**(4), 497-503.

Kim, Y.T., Lee, C. and Park, H.I. (2011), "Experimental study on engineering characteristics of composite geomaterial for recycling dredged soil and bottom ash", *Mar. Georesour. Geotech.*, **29**(1), 1-15.

Kisi, O. (2008), "The Potential of different ANN techniques in evapotranspiration modeling", *Hydrol. Processes*, **22**(14), 2449-2460.

Kisi, O. (2009), "Daily pan evaporation modelling using multi-layer perceptrons and radial basis neural networks", *Hydrol. Processes*, **23**(2), 213-223.

Kisi, O. and Cobaner, M. (2009), "Modeling river stage-discharge relationships using different neural network computing techniques", *Clean Soil Air Water*, **37**(2), 160-169.

Kisi, O. and Fedakar, H.I. (2014), "Modeling of suspended sediment concentration carried in natural streams using fuzzy genetic approach", *Comput. Intell. Tech. Earth Environ. Sci.*, 175-196.

Kiszka, J.B., Kochanskia, M.E. and Sliwinska, D.S. (1985), "The influence of some fuzzy implication operators on the accuracy of fuzzy model-part II", *Fuzzy Sets Syst.*, **15**(3), 223-240.

Kocabas, F. and Unal, S. (2010), "Compared techniques for the critical submergence of an intake in water flow", *Adv. Eng. Softw.*, **41**(5), 802-809.

Lambe, T.W. and Kaplar, T.W. (1971a), "Additives for modifying the frost susceptibility of soils", Technical Report No. 123, Part 1, USA Cold Regions Research and Engineering Laboratory, Hanover, NH, USA.

Lambe, T.W., Kaplar, C.W. and Lambe, T.J. (1971b), "Additives for modifying the frost susceptibility of soils", Technical Report No. 123; Part 2, USA Cold Regions Research and Engineering Laboratory, Hanover, NH, USA.

Lee, G.C. and Chang, S.H. (2003), "Radial basis function networks applied to DNBR calculation in digital core protection systems", *Ann. Nucl. Energy*, **30**(15), 1561-1572.

Lee, S.J., Lee, S.R. and Kim, Y.S. (2003), "An approach to estimate unsaturated shear strength using artificial neural network and hyperbolic formulation", *Comput. Geotech.*, **30**(6), 489-503.

Leonard, J.A., Kramer, M.A. and Unga, L.H. (1992), "Using radial basis functions to approximate a function and its error bounds", *IEEE Trans. Neural Netw.*, **3**(4), 624-627.

Levine, E.R., Kimes, D.S. and Sigillito, V.G. (1996), "Classification soil structure using neural networks", *Ecol. Model.*, **92**(1), 101-108.

Looney, C.G. (1996), "Advances in feed-forward neural networks: demystifying knowledge acquiring black boxes", *IEEE Trans. Knowl. Data. Eng.*, **8**(2), 211-226.

Marquardt, D. (1963), "An algorithm for least squares estimation of non-linear parameters", *J. Soc. Ind. Appl. Math.*, **11**(2), 431-441.

Modi, O.P., Mondal, D.P., Prasad, B.K., Singh, M. and Khaira, H.K. (2003), "Abrasive wear behavior of high carbon steel: Effects of microstructure and experimental parameters and correlation with mechanical properties", *Mater. Sci. Eng.:A*, **343**(1-2), 235-242.

Murray, T. and Farrar, M. (1988), "Temperature distributions in reinforced soil retaining walls", *Geotext. Geomembr.*, **7**(1-2), 33-50.

Najjar, Y.M., Basheer, I.A. and Naous, W.A. (1996), "On the identification of compaction characteristics by neuronets", *Comput. Geotech.*, **18**(3), 167-187.

Narendra, B.S., Sivapullaiah, P.V., Suresh, S. and Omkar, S.N. (2006), "Prediction of unconfined compressive strength of soft grounds using computational intelligence techniques: A comparative study", *Comput. Geotech.*, **33**(3), 196-208.

Poggio, T. and Girosi, F. (1990), "Regularization algorithms for learning that are equivalent to multilayer networks", *Sci.*, **247**(4945), 978-982.

Rifai, A., Yasufuku, N. and Tsuji, K. (2009), "Characterization and effective utilization of coal ash as soil stabilization on road application", In: (C.F. Leung, J. Chu and R.F. Shen Eds.), *Ground Improvement*

Technologies and Case Histories, Research Publishing Services, pp. 469-474.

Rumsey, D.J. (2011), *Statistics for Dummies*, (2nd Edition), John Wiley & Sons, NJ, USA.

Shahin, M.A., Jaksa, M.B. and Maier, H.R. (2001), "Artificial neural network applications in geotechnical engineering", *Aust. Geomech.*, **36**(1), 49-62.

Shahin, M.A., Maier, H.R. and Jaksa, M.B. (2003), "Settlement prediction of shallow foundations on granular soils using B-spline neurofuzzy models", *Comput. Geotech.*, **30**(8), 637-647.

Sinha, S.K. and Wang, M.C. (2008), "Artificial neural network prediction models for soil compaction and permeability", *Geotech. Geol. Eng.*, **26**(1), 47-64.

Sivapullaiah, P.V., Guru Prasad, B. and Allam, M.M. (2009), "Modeling sulfuric acid induced swell in carbonate clays using artificial neural networks", *Geomech. Eng., Int. J.*, **1**(4), 307-321.

Sivrikaya, O., Kiyildi, K.R. and Karaca, Z. (2014), "Recycling waste from natural stone processing plants to stabilise clayey soil", *Environ. Earth Sci.*, **71**(10), 4397-4407.

Specht, D.F. (1991), "A general regression neural network", *IEEE Trans. Neural Netw.*, **2**(6), 568-576.

Stegemann, J.A. and Buenfeld, N.R. (2003), "Prediction of unconfined compressive strength of cement paste containing industrial wastes", *Waste Manag.*, **23**(4), 321-332.

Tsoukalas, L.H. and Uhrig, R.E. (1997), *Fuzzy and Neural Approaches in Engineering*, Wiley, NY, USA.

Tutumluer, E. and Seyhan, U. (1998), "Neural network modeling of anisotropic aggregate behavior from repeated load triaxial tests", *J. Transport. Res. Board*, **1615**, 86-93.

Tutumluer, E., Santoni, R.L. and Kim, I.T. (2004), "Modulus anisotropy and shear stability of geofiber-stabilized sands", Transportation Research Board, National Research Council; Transportation Research Record 1874, Washington, D.C., USA, pp. 125-135.

Unal, B., Mamak, M., Seckin, G. and Cobaner, M. (2010), "Comparison of an ANN approach with 1-D and 2-D methods for estimating discharge capacity of straight compound channels", *Adv. Eng. Softw.*, **41**(2), 120-129.

Wasserman, P.D. (1993), *Advanced Methods in Neural Computing*, Van Nostrand Reinhold, NY, USA.

Yilmaz, I and Kaynar, O. (2011), "Multiple regression, ANN (RBF, MLP) and ANFIS models for prediction of swell potential of clayey soils", *Expert Syst. Appl.*, **38**(5), 5958-5966.

Zaimoglu, A.S. (2010), "Freezing-thawing behavior of fine-grained soils reinforced with polypropylene fibers", *Cold Reg. Sci. Technol.*, **60**(1), 63-65.

CC